Using Densely Distributed Soil Moisture Observations for Calibration of a Hydrologic Model

ANDREA THORSTENSEN

Department of Civil and Environmental Engineering, University of California, Irvine, Irvine, California

PHU NGUYEN

*Department of Civil and Environmental Engineering, University of California, Irvine, Irvine, California,
and Nong Lam University, Ho Chi Minh City, Vietnam*

KUOLIN HSU AND SOROOSH SOROOSHIAN

Department of Civil and Environmental Engineering, University of California, Irvine, Irvine, California

(Manuscript received 1 May 2015, in final form 8 October 2015)

ABSTRACT

Calibration is a crucial step in hydrologic modeling that is typically handled by tuning parameters to match an observed hydrograph. In this research, an alternative calibration scheme based on soil moisture was investigated as a means of identifying the potentially heterogeneous calibration needs of a distributed hydrologic model. The National Weather Service's (NWS) Hydrology Laboratory Research Distributed Hydrologic Model (HL-RDHM) was employed to carry out such a calibration, along with concentrated in situ soil moisture observations from the Iowa Flood Studies (IFloodS) field campaign in Iowa's Turkey River basin. Synthetic, single-pixel experiments were conducted in order to identify parameters relevant to soil moisture dynamics and to test the ability of three calibration procedures (discharge, soil moisture, and hybrid based) to recapture prescribed parameter sets. It was found that three storage parameters of HL-RDHM could be consistently identified using soil moisture RMSE as the objective function and that the addition of discharge-based calibration led to more consistent parameter identification for all 11 storage and release parameters. Expanding to full-basin experiments, these three calibration procedures were applied following an investigation to find the most advantageous method of distributing the point-based calibrations carried out at each pixel collocated with an IFloodS observation site. A method based on pixel similarity was deemed most appropriate for this purpose. Additionally, streamflow simulations calibrated with soil moisture showed improvement in RMSE and Nash–Sutcliffe efficiency (NSE) for all calibration–validation events despite a short calibration period, a promising result when considering calibration of ungauged basins. However, supplementary evaluation metrics show mixed results for streamflow simulations, suggesting further investigation is required.

1. Introduction

For many years, calibration of hydrologic models has been a crucial step in identifying parameters used to represent mechanisms that are either poorly understood, too computationally expensive to resolve, or even unnecessary for a given application. Calibration of hydrologic models has traditionally been performed by adjusting model parameters such that the simulated hydrograph best fits an observed hydrograph. This framework is often limited in that the observed outlet hydrograph is the result of a collection of many internal basin processes (Ivanov et al. 2010; Liang and Xie 2001). Several studies have pointed to soil moisture as a possible vehicle for describing these heterogeneous subbasin processes, particularly in respect to how streamflow is modulated (Santanello et al. 2007; Campo et al. 2006; Wanders et al. 2014; Zamora et al. 2014). Some have turned to other variables such as evapotranspiration (Rientjes et al. 2013; Immerzeel and Droogers 2008; Cao

Corresponding author address: Andrea Thorstensen, Dept. of Civil and Environmental Engineering, University of California, Irvine, E/4130 Engineering Gateway, Office EH 5308, Mail Code 2175, Irvine, CA 92697.
E-mail: athorste@uci.edu

et al. 2006), snow-covered area (Isenstein et al. 2015; Franz and Karsten 2013), and nitrogen concentration (Bergström et al. 2002) in lieu of, or as a compliment to, calibrating to discharge. While significant progress has been made from these studies, challenges still remain regarding how best to leverage available observations for calibration.

In an effort to accommodate the ever-growing need to represent subbasin processes, the development of distributed hydrologic and land surface models (LSMs) has become an area of great interest. Some of these models are physically based, with a realistically meaningful structure of soil layers. Such models include the Noah land surface model (Chen et al. 1996) and the Soil–Water–Atmosphere–Plant (SWAP) model (van Dam et al. 1997). Others feature a more conceptual representation of soil layers in the rainfall–runoff generation process, such as the Variable Infiltration Capacity model (VIC; Wood et al. 1992), NOAA/National Weather Service (NWS) Hydrology Laboratory Research Distributed Hydrologic Model (HL-RDHM; Koren et al. 2004), the U.S. Army Corps of Engineers' Gridded Surface Subsurface Hydrologic Analysis model (Downer and Ogden 2004), and the LISFLOOD model (van der Knijff et al. 2010). As they are distributed in nature, all of these models have the opportunity to incorporate soil moisture information to improve representation of internal basin processes. Several studies have investigated use of soil moisture observations in distributed models for this very purpose (e.g., Das et al. 2008; Hsu et al. 2012; Wanders et al. 2014). Those models that are conceptually based and rely on parameterizations of soil processes may also benefit from soil moisture observations as a way to calibrate those parameters that control subbasin mechanisms.

As the capabilities for observing soil moisture progress, the feasibility for use in the aforementioned distributed hydrologic models improves. Several in situ soil moisture–monitoring networks have been providing local soil moisture measurements for years. As part of the Oklahoma Mesonet (Brock et al. 1995), soil moisture–monitoring instruments have been deployed since 1996 (Scott et al. 2013). The NOAA Hydrometeorology Testbed program has developed soil moisture observation networks in the Russian River and North Fork American River basins in California as well as the San Pedro River basin in Arizona (Zamora et al. 2011). Since the 1990s, the U.S. Department of Agriculture (USDA) Natural Resources Conservation Service has hosted the Soil Climate Analysis Network (SCAN), a continental-scale network with over 100 stations across the United States (Schaefer et al. 2007). The Walnut Gulch Experimental Watershed housed 19 near-surface soil moisture measurement instruments from 2002 to 2006 in addition to a select few sites with deeper soil profile measurements and longer record periods (Keefer et al. 2008). Recent years have witnessed the extension from ground-based observations to retrievals from satellites. The European Space Agency's Soil Moisture Ocean Salinity (SMOS) satellite mission was launched in 2009 with the purpose of measuring sea surface salinity over the world's oceans and surface soil moisture over land (Kerr et al. 2010). The recently launched Soil Moisture Active Passive (SMAP) mission from the National Aeronautics and Space Administration (NASA) utilizes a passive L-band radiometer combined with active L-band radar (Entekhabi et al. 2010). Distributed hydrologic modeling lends itself nicely to such observations, as they can account for the subbasin soil moisture variations. In support of the NASA Global Precipitation Measurement (GPM) validation efforts, the Iowa Flood Center (IFC) launched the Iowa Flood Studies (IFloodS) field campaign in the spring of 2013. As part of the comprehensive collection of hydrometeorological instrumentation used for IFloodS, 20 soil moisture probe sites were deployed in a catchment in northeastern Iowa (Krajewski et al. 2013). While limited in observation period length, these observations are rich in terms of spatial density.

Utilization of soil moisture observations as a tool for calibrating hydrologic models has been explored in several studies. Wanders et al. (2014) propose the use of satellite-based surface soil moisture observations in conjunction with discharge observations in a dual state or parameter estimation of the LISFLOOD model in the upper Danube. This study found an improvement of discharge simulations when both observations were used for calibration over using discharge-only-based calibration and that there was the added benefit of improved soil moisture simulation throughout the catchment. Campo et al. (2006) use synthetic aperture radar data to infer information about soil moisture at bare soil pixels to use for calibration of the distributed hydrologic model Mobile Digital Computer (MOBIDIC). Although restricted to areas with little to no vegetation cover, results of this work also demonstrate improvement in simulated discharge with the addition of soil moisture–based calibration. Studies using limited in situ observations for basin calibration have found some improvement in discharge simulations. Koren et al. (2008) explore the calibration of basin-average soil moisture for HL-RDHM. Using daily, basin-average soil moisture calibration, simulated discharge improvement was achieved by defining an objective function that took into account the root-mean-square error (RMSE) of outlet streamflow at four different time scales combined with RMSE of two soil moisture layers.

In this study, using the NWS HL-RDHM, a distributed calibration approach based on soil moisture is developed. This approach allows the loosening of the assumption in Koren et al. (2003) that states a priori parameter gridcell values are correctly proportioned relative to one another. This soil moisture–based calibration is tested alongside the traditional discharge-based calibration, and a two-step hybrid scheme is introduced. Pixel-scale synthetic studies are carried out to identify appropriate parameters for soil moisture–based calibration and to evaluate performance under ideal conditions (all inputs and outputs are known as well as the corresponding parameter sets that produce them). These single-pixel experiments are then expanded to the full-basin scale for a basin that is included in the IFloodS experiment domain. This study aims to 1) determine which HL-RDHM parameters are most identifiable when calibrating to soil moisture, 2) test how to best spread calibration information from isolated pixels to the full-basin scale so that internal basin process representation is enhanced, and 3) examine if the inclusion of soil moisture observations in the calibration process provides additional improvement to streamflow simulations or if it can improve streamflow simulations as a standalone under the circumstance that streamflow observations are unavailable.

2. Model and methods

a. HL-RDHM description

HL-RDHM was developed by the NWS/Office of Hydrologic Development (OHD). Detailed information can be found in Koren et al. (2004), NWS (2011), and Smith et al. (2012). HL-RDHM is a distributed hydrologic model that was designed and implemented for the entire contiguous United States (CONUS) at three spatial resolutions of 1 Hydrologic Rainfall Analysis Project (HRAP; ~4 km), ½ HRAP, and ¼ HRAP. HL-RDHM structure can also be applied for any cell resolution and time step length (NWS 2011). The heart of the model is the Sacramento Soil Moisture Accounting (SAC-SMA) with Heat Transfer Component (SAC-HT). In SAC-HT, unlike other distributed models with fixed values for subdomains or the entire domain, an advanced algorithm was designed to derive a priori parameters from soil and land-use data. Recent enhancements to the basic SAC-SMA model include the use of Noah LSM–based physics to estimate a physically meaningful soil moisture profile as well as evapotranspiration from the soil column. This is accomplished through the conversion of SAC-SMA conceptual soil water storages into physical soil layers. Once this is done, a heat transfer component accounting for frozen ground processes allows
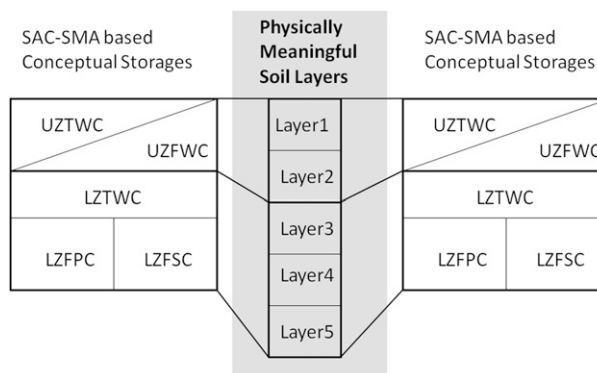

FIG. 1. Example conversion of SAC-SMA conceptual storages to model-prescribed physically meaningful soil layers (number of layers varies from pixel to pixel).

the soil liquid and solid water contents at each soil layer to be estimated (Koren et al. 2007).

Utilizing the Noah LSM vegetation–soil moisture interaction parameterization as well as datasets regarding vegetation activities, Koren et al. (2010) have further adjusted SAC-HT soil moisture estimations at different physical layers through advancing the evapotranspiration (ET) estimation in SAC-HT by accounting for the effects of photosynthetically active radiation, soil moisture and vapor pressure deficits, and air temperature on ET. Empirical relationships are used to estimate these additional variables in an effort to reduce input data requirements to a level consistent with what is available for River Forecast Center operations. This new version is referred to as the SAC-HT for Enhanced Evapotranspiration (SAC-HTET) and is included in HL-RDHM, version 3.2.1 (used in this study). After the soil moisture is adjusted at different physical layers, it is shuffled backed to SAC-SMA conceptual layers (see Fig. 1) where adjustments due to free water exchange and removal from runoff are made.

An optional HL-RDHM routine that was utilized in this study is the rutpix9 routing module. This module has a hillslope component, where surface and subsurface flows are routed over a uniform conceptual hillslope. In the channel-routing component of rutpix9, water moves from cell to cell according to a predefined cell connectivity sequence. This sequence is topography based such that at each cell, fast runoff routed over the hillslope of that cell is combined with the subsurface flow and streamflow routed from the upstream pixels (NWS 2011).

This study also employs the snow component in HL-RDHM known as SNOW17. This routine uses empirical relationships to calculate heat storages, liquid water storages, and snowpack melt to represent snow accumulation and ablation (Anderson 1973). Although all evaluation periods of this study occur during springs and summers

TABLE 1. HL-RDHM parameters considered for calibration and feasible ranges as provided by Koren et al. (2008).

Parameter	Description	Range
SAC-HTET		
UZTWM	Upper-zone tension water max (mm)	10–300
UZFWM	Upper-zone free water max (mm)	5–150
UZK	Upper-zone free water depletion rate due to interflow (day^{-1})	0.10–0.75
ZPERC	Max and min percolation rate ratio	5–350
REXP	Percolation curve shape parameter	1–5
LZTWM	Lower-zone tension water max (mm)	10–500
LZFSM	Lower-zone supplemental free water max (mm)	5–400
LZFPM	Lower-zone primary free water max (mm)	10–1000
LZSK	Lower-zone supplemental free water depletion rate due to interflow (day^{-1})	0.01–0.35
LZPK	Lower-zone primary free water depletion rate due to interflow (day^{-1})	0.001–0.05
PFREE	Fraction of percolated water that goes straight to lower-zone free storage	0.0–0.8
rutpix9		
Q0CHN	Channel specific discharge (m s^{-1})	
QMCHN	Power value for discharge cross-sectional relationship	
ROUGH	Hillslope roughness coefficient	
SLOPH	Hillslope slope	

that are snow-free, the model spinup periods include the preceding winters of each event in this research. No parameters from the SNOW17 module were included in the calibration process, as the focus of this study is to investigate the potential of soil moisture. Because soil water is likely to be frozen during the time periods when SNOW17 would be activated, soil moisture evolution is rendered unusable for calibration of the snow module parameters in this research.

The 11 SAC-HTET storage and release parameters and four rutpix9 routing parameters that are calibrated for this study are presented in Table 1. The feasible ranges for the storage and release parameters proposed by Koren et al. (2008) are also provided in this table. These ranges were used as bounds during calibration. For all simulations, calibration or validation, a 1-yr spinup period was used. The model was run at an hourly time step, with a 1 HRAP spatial resolution (~4 km).

b. Calibration scheme

Calibration of HL-RDHM was performed with the global search algorithm, Shuffled Complex Evolution–University of Arizona (SCE-UA; Duan et al. 1992). Use of SCE-UA and its subsequent variations have been extensively used in hydrologic modeling (Sorooshian et al. 1993; Duan et al. 1994; Gan and Biftu 1996; Cooper et al. 1997, 2007; Hogue et al. 2000, 2003; Vrugt et al. 2003b; Chu et al. 2010; Zhang et al. 2015). The notion of multiobjective strategies for hydrologic modeling has been highlighted in Gupta et al. (1998), Yapo et al. (1998), Vrugt et al. (2003a), and Shafii and De Smedt (2009), among others. These studies emphasize the need to exploit as much useful information as possible from observations rather than relying on a single objective.

This can be in the form of calibrating to multiple variables, or calibrating to multiple signals of the same variable. With this in mind, the calibration scheme here focuses on soil moisture and discharge as the two calibration variables. For the soil moisture–based calibration of this work, SCE-UA was applied at the single-model pixel scale, wherever in situ soil moisture observations were available. The objective function to minimize in this case was the combined RMSE of four observed soil moisture layers. For discharge-based calibration in this study, the objective function that SCE-UA sought to minimize was the RMSE of simulated discharge.

Hogue et al. (2000, 2003) introduced an automatic calibration scheme for the lumped version of SAC-SMA and SNOW17 that was designed to mimic the manual calibration approach of NWS. This method featured two objective functions used in successive calibration, with each objective function targeting specific parameters (i.e., baseflow parameters with one objective function, upper-zone parameters with the second). Franz and Karsten (2013) explore a multistep calibration process that targets parameters in the SNOW17 model where three parameters are first optimized to snow-covered area followed by an additional parameter being optimized via streamflow observations and simulations from the lumped SAC-SMA. The work presented here similarly explores stepwise calibration of a watershed that focuses on relevant parameters by following the example of Franz and Karsten (2013) of targeting certain parameter groups with different variables. Soil moisture observations from the IFloodS experiment are used to calibrate a specific parameter group followed by discharge-based calibration of the remaining parameters. The effects of only using soil moisture–based

calibration and discharge-only-based calibration are also investigated.

The framework for the soil moisture–based calibration of this study relies on calibrating single pixels within the distributed model domain, but dispersing the calibration to the rest of the model pixels. To apply parameter adjustment of the individually calibrated parameters to the rest of the pixels in the basin, three different distribution schemes were investigated:

- Inverse distance weighting (InvDist): Inverse distance weighting of parameters was used to distribute calibrated values to neighboring pixels according to physical proximity. Weights for InvDist are calculated as

$$w_i(\mathbf{x}) = \frac{1}{d(\mathbf{x},\mathbf{x}_i)^p}$$

$$d(\mathbf{x},\mathbf{x}_i) = \sqrt{\sum_{j=1}^{n}(x_j - x_{ij})^2}, \tag{1}$$

where w_i is the weight of the ith calibrated pixel given to the unknown pixel $\mathbf{x}$, based on the distance d, between pixel $\mathbf{x}$ and calibrated pixel $\mathbf{x}_i$, and p is the power parameter (chosen as 2 for this study). Parameter values are then assigned to pixel $\mathbf{x}$ as

$$\boldsymbol{\theta}(\mathbf{x}) = \begin{cases} \dfrac{\displaystyle\sum_{i=1}^{N} w_i(\mathbf{x})\boldsymbol{\theta}(\mathbf{x}_i)}{\displaystyle\sum_{i=1}^{N} w_i(\mathbf{x})} & \text{if} \quad d(\mathbf{x},\mathbf{x}_i) \neq 0 \\[4mm] \boldsymbol{\theta}(\mathbf{x}_i) & \text{if} \quad d(\mathbf{x},\mathbf{x}_i) = 0 \end{cases}, \tag{2}$$

where $\boldsymbol{\theta}(\mathbf{x})$ is a vector of parameters at pixel $\mathbf{x}$ and $\boldsymbol{\theta}(\mathbf{x}_i)$ is a vector of parameters at calibrated pixel $\mathbf{x}_i$.

- Similarity of pixels weighting (SimPix): SimPix is a distribution method based on the similarity of pixel characteristics and was created following the InvDist method with the exception that the distance is now defined as the Euclidean distance in parameter space rather than in 2D physical space:

$$d(\boldsymbol{\theta}'_{\mathbf{x}},\boldsymbol{\theta}'_{\mathbf{x}_i}) = \sqrt{\sum_{k=1}^{m}\left(\frac{\theta_{\mathbf{x}_k} - \theta'_{\mathbf{x}_{ik}}}{\theta_{k_{\mathrm{MAX}}} - \theta_{k_{\mathrm{MIN}}}}\right)^2}, \tag{3}$$

where $\boldsymbol{\theta}'_{\mathbf{x}}$ is the uncalibrated parameter vector at pixel $\mathbf{x}$, $\boldsymbol{\theta}'_{\mathbf{x}_i}$ is the uncalibrated parameter vector at calibrated pixel $\mathbf{x}_i$, and $\theta_{k_{\mathrm{MAX}}}$ and $\theta_{k_{\mathrm{MIN}}}$ are the maximum and minimum value of the kth parameter, respectively. The $(\theta_{k_{\mathrm{MAX}}} - \theta_{k_{\mathrm{MIN}}})$ term is a necessary regularization provision that prevents the magnitude of a given parameter from dominating the similarity measure.

This method was developed using the a priori parameter grids provided by the NWS as the metric of similarity, given that these parameter grids are derived from soil surveys (Koren et al. 2003). It is assumed that if a specific pixel requires calibration, those pixels that are physically similar according to the a priori parameters will need to be calibrated similarly. This has the potential advantage over the InvDist method in that the unobservable pixels do not need to be in the near vicinity of the observable pixels and that a landscape with drastically changing soil characteristics in space will not become smoothed by the InvDist process.

- Basic average of scalar multipliers (BaseAve): The BaseAve method follows the same assumptions as the original calibration method outlined in NWS (2011). In this method, scalar multipliers are identified and applied to the a priori parameter grids while presupposing that the spatial relationship of the parameters is correct and that only their average magnitude requires adjustment. To identify basin multipliers in this study, a multiplier is calculated for each parameter at every observation station pixel, and the average of the multipliers is taken and applied to the original grids basinwide. Like its discharge-based calibration counterpart that is traditionally used and is discussed in NWS (2011), this distribution method will see no changes in the description of basin heterogeneity beyond what has already been established in the a priori parameter grids.

c. Performance metrics

The model was evaluated using five metrics: RMSE, bias, correlation (CORR), coefficient of determination R^2, and Nash–Sutcliffe efficiency (NSE). RMSE is defined by

$$\mathrm{RMSE} = \sqrt{\frac{1}{n}\sum_{t=1}^{n}[o(t) - s(t)]^2}, \tag{4}$$

where n is the total number of observations, o is the observed variable, and s is the corresponding simulated variable for each time step t ($t = 1\,\mathrm{h}$ for all cases in this study).

Bias indicates the tendency of the simulated soil moisture and streamflow in comparison with observations. The ideal value of bias is zero. Positive values of bias indicate a tendency to overestimate while negative values indicate an underestimation:

$$\mathrm{bias} = \frac{\displaystyle\sum_{t=1}^{n}[s(t) - o(t)]}{\displaystyle\sum_{t=1}^{n} o(t)}. \tag{5}$$
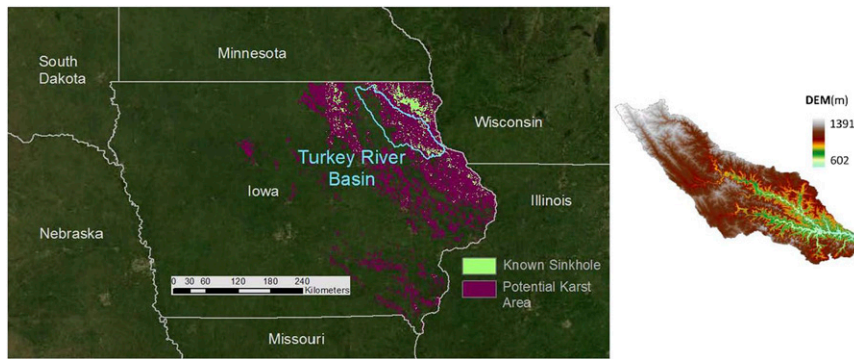
FIG. 2. (left) Turkey River basin and Iowa's karstic regions. (right) Topography of Turkey River basin derived from 30-m DEM.

CORR is one of the most commonly used measures for evaluating the goodness of fit of simulated and observed time series data arrays. CORR ranges from -1 (perfectly negatively correlated) to 1 (perfectly positively correlated). The ideal value of CORR is 1 and CORR of 0 indicates no correlation between the simulation and observation:

$$\text{CORR} = \frac{\sum_{t=1}^{n}[o(t)-\overline{o}]\sum_{t=1}^{n}[s(t)-\overline{s}]}{\sqrt{\sum_{t=1}^{n}[o(t)-\overline{o}]^2}\sqrt{\sum_{t=1}^{n}[s(t)-\overline{s}]^2}}. \quad (6)$$

Coefficient of determination indicates how well measured data fit a statistical model. The R^2 ranges from 0 to 1, with acceptable values greater than 0.5 (Moriasi et al. 2007). It is calculated as the square of the CORR.

NSE is a commonly used metric in hydrologic modeling, which indicates the fitness of the simulated discharge with the observed hydrograph. NSE ranges from $-\infty$ to 1. The ideal value of NSE is 1. Negative NSE indicates that the simulated value is worse than the mean of the observations:

$$\text{NSE} = 1 - \frac{\sum_{t=1}^{n}[s(t)-o(t)]^2}{\sum_{t=1}^{n}[o(t)-\overline{o}]^2}. \quad (7)$$

3. Study area and data

a. Study area

The Turkey River (Fig. 2) is a 246-km tributary of the upper Mississippi River covering a drainage area of 4384 km^2 in Iowa. The region is composed primarily of nonirrigated farmland (corn and soybeans). Northeastern Iowa, where the Turkey River basin is located, hosts an area characterized by a karstic and high-relief landscape. These complex systems allow for the rapid transmission of groundwater through broken rocks, eventually leading to steeply banked streams through seeps and springs (Libra 2005). While the conceptual rainfall–runoff scheme does not explicitly represent a water table, the lower zone incorporates the saturated zone (Brazil and Hudlow 1981), which may be influenced by the karst formations. The sinkholes that pepper this region allow surface runoff to directly infiltrate to the water table (Libra 2005). This particular geological formation is not directly accounted for in HL-RDHM and adds a unique complication to the experiment, particularly in the southeastern region of the basin, where there is a concentration of known sinkholes.

The IFloodS campaign was carried out as a ground validation component of the GPM project (Krajewski et al. 2013; Demir et al. 2015; Schwaller and Morris 2011; Tapiador et al. 2012). IFloodS provided multiple real-time observed hydrometeorological data during spring of 2013 from tipping-bucket rain gauges, weather radars, streamflow and stage gauges, and soil moisture probes. The campaign provides a unique opportunity for hydrologic modeling studies using high-quality data from the dense observation network.

b. Data

The two primary data components required for this study were soil moisture and discharge. The soil moisture data used are from the IFloodS field campaign. These data are available at 5-, 10-, 20-, and 50-cm depths at 20 in situ locations throughout the Turkey River basin during the spring of 2013. Figure 3 depicts the layout of
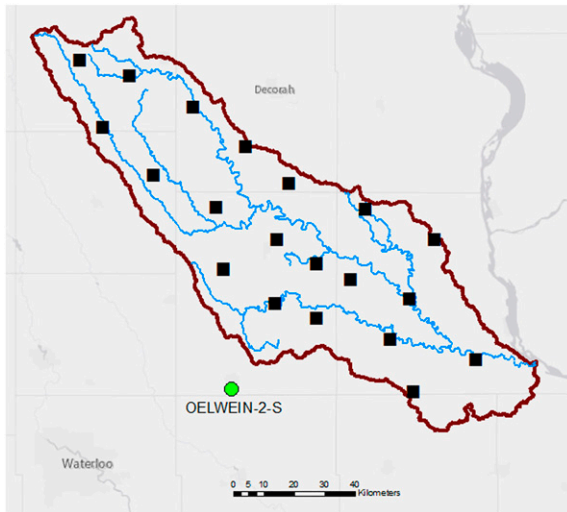
FIG. 3. IFloodS network of in situ soil moisture observations (squares) in the Turkey River basin and the NWS COOP site OELWEIN-2-S (circle).

the IFloodS soil moisture network. Station soil moisture time series were averaged from 15 min to hourly observations for use in this study. Basin outlet discharge data used were from the USGS streamflow gauge number 05412500 at Garber, Iowa. These too were averaged from 15 min to hourly data to remain consistent with model simulations. All nonsynthetic experiments for calibration and soil moisture–based validation in this study are set up from 24 April to 24 June 2013, a time period in which data are available from the IFloodS campaign.

HL-RDHM requires two types of forcing data: precipitation and temperature. This research used the National Centers for Environmental Prediction (NCEP) NEXRAD stage IV rainfall data derived from multiple sensors (gauges and radars) over the CONUS. The reanalysis air temperature from phase 2 of the North American Land Data Assimilation System (NLDAS-2) available from NASA Goddard Earth Sciences Data and Information Services Center (GES DISC) was also used. Both forcing data are in 4-km, hourly, spatiotemporal resolution.

This study also makes use of data from the NWS Cooperative Observer (COOP) program. The NWS COOP is made of a network of over 7000 volunteer climate data observers in addition to the hundreds of NWS stations. These sites record daily maximum and minimum temperatures as well as precipitation to aid in the study of various climate phenomena in the United States (Robinson 1990). Daily precipitation from the COOP site OELWEIN-2-S (Fig. 3) in northeastern Iowa was utilized in the synthetic study design (described in the following section).

4. Synthetic single-pixel experiment

a. Synthetic single-pixel experiment setup

To evaluate the suitability of using soil moisture data to identify parameters in HL-RDHM, single-pixel synthetic studies were conducted. Use of a single pixel reduces the complexity of a fully distributed basin and allows for a simple, ideal case representation of the larger experiment. These single-pixel experiments were carried out in two phases: 1) a sensitivity analysis of all parameters plausibly relevant to soil moisture and 2) a series of scenarios that test the ability to retrieve a prescribed parameter set.

A model pixel located near the Turkey River basin extent was selected for the synthetic experiments. Within this pixel is the NWS COOP site OELWEIN-2-S, which has a data record that dates back to 1951. Climate data from this site were used to design 2-month-long synthetic precipitation patterns of varying intensity. The temporal pattern was taken as the basin average of the May–June 2005 precipitation stage IV hourly estimates. This pattern was linearly scaled such that the total precipitation equals the minimum, median, and high May–June precipitation totals from the COOP site. NLDAS-2 temperatures from the same 2005 time period that the precipitation was based on were used to force the model in all three scenarios. The a priori parameter values from the NWS at this pixel were taken as the prescribed true parameters. This was done to ensure a realistic combination of the parameters, as several studies have demonstrated reasonable simulations using the a priori parameter sets (e.g., Nguyen et al. 2015; Fares et al. 2014). It should be emphasized that calibration of HL-RHDM parameters in the upper Midwest has been shown to substantially improve simulation results (Spies et al. 2015), and that use of the a priori sets for this synthetic study is simply to provide a plausible mixture of parameters. The model was run using the a priori parameters, and the resulting simulated soil moisture at the four observable layers of the IFloodS instruments and simulated pixel discharge were used as "perfect observations" to complete the ideal case experiments.

b. Synthetic single-pixel experiment results

1) SENSITIVITY ANALYSIS

Each of the 11 SAC-HTET parameters related to storage and release were perturbed one at a time to evaluate individual effects on soil moisture and discharge (at the single-pixel scale). The entire plausible range for each parameter as provided in Koren et al. (2008) was explored (see Table 1). The median precipitation scenario described in the previous
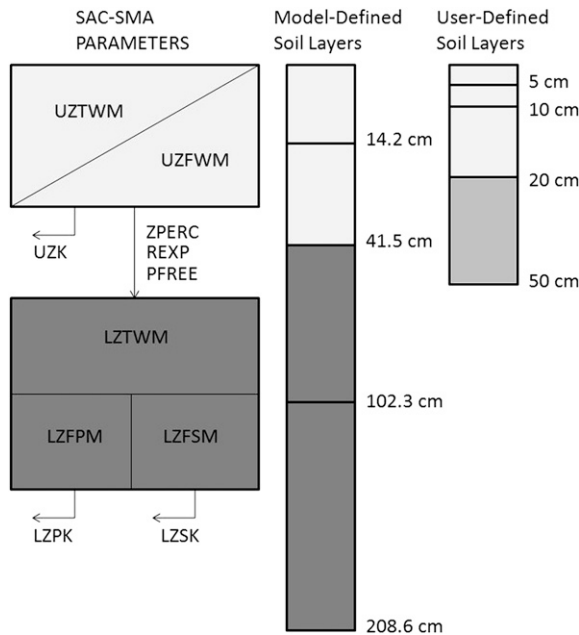
FIG. 4. Sample (pixel at NWS COOP site OELWEIN-2-S) connection between the SAC-SMA conceptual storage parameters, model-defined soil layers, and user-defined soil layers. Light shades correspond to the upper-zone conceptual storages, dark shades to lower-zone storages, and the medium shade lies in both.

section was used to drive the model. An example conceptualization of how the in situ observations in this study relate to the model parameters is provided in Fig. 4. Although the exact relationship will vary from pixel to pixel, this example shows the parameter–soil layer relationship of the synthetic experiment pixel, which provides an idea of how parameters of pixels in the Turkey River basin are related to the IFloodS soil moisture observation layers. The model defines its own layers for internal calculations while offering the user the ability to request specific layers, which are interpolated from the model-defined soil layers.

Figure 5 qualitatively shows the sensitivity of simulated soil moisture at the four observable soil layers for the IFloodS campaign. Of the 11 parameters, the storage parameters (UZTWM, UZFWM, LZTWM, LZFSM, and LZFPM; see Table 1 for definitions) exhibit sensitivity in the simulated soil moisture at all four layers, as seen as a spread in the soil moisture estimate with changing parameter values. The three free water storage parameters show lower soil moisture estimates when lower parameter values are used, and the two tension water storage parameters show higher soil moisture estimates at the lower end of the parameter spectrum. UZFWM displays the highest

sensitivity for the lower parameter values, whereas the other four storage parameters are more sensitive in the higher range.

Sensitivity of discharge response to changing the same suite of parameters was also examined (Fig. 6). For this experiment, single-pixel runoff is considered to be ''discharge,'' as there is no channel flow or routing during this step. Unlike the soil moisture signature, discharge exhibits some degree of sensitivity to all of the parameters under consideration. This figure demonstrates the potential complications of changing several SAC-HTET parameters simultaneously while using the discharge pattern as the evaluation tool for pursuing the ''true'' parameter values. For example, the discharge has an exceptionally similar response to the range of possible values for LZTWM, LZSK, and LZPK. The response for changing UZK also has the same shape, but opposite effect with changing parameter magnitude. It follows that there may not be sufficient information to adjust certain observed hydrograph behaviors via the proper parameter during discharge-based calibration.

2) PARAMETER IDENTIFICATION TESTS

To test the ability to recapture predefined parameter values at the pixel scale, SCE-UA calibration was implemented 15 separate times (five times for each of the three different precipitation intensity patterns). This was done for three cases, each defined by a different objective function. All 11 storage and release parameters were allowed to be calibrated, and it was assumed that no prior information of the parameters was available so that the entire parameter space defined by the bounds in Table 1 can be explored.

For the first case, RMSE of the four observable soil moisture layers was used as the targeted objective function to minimize. Figure 7 shows the results of this soil moisture–based calibration in the normalized parameter space (gray markers). The results show that UZTWM, UZFWM, and LZTWM are well identified by soil moisture calibration when forced with any of the three precipitation intensities. The lower-zone free storage parameters (LZFSM and LZFPM) showed a moderate spread in estimated parameter location from the 15 trials, and the remainder of the parameters showed a large spread, suggesting soil moisture–based calibration may be unreliable in their identification. The next case followed the same setup as the first, with the exception of utilizing discharge RMSE for the objective function. This scenario shows some degree of spread in estimated parameters for all cases. However, it can be seen that for the highest precipitation intensity trials,
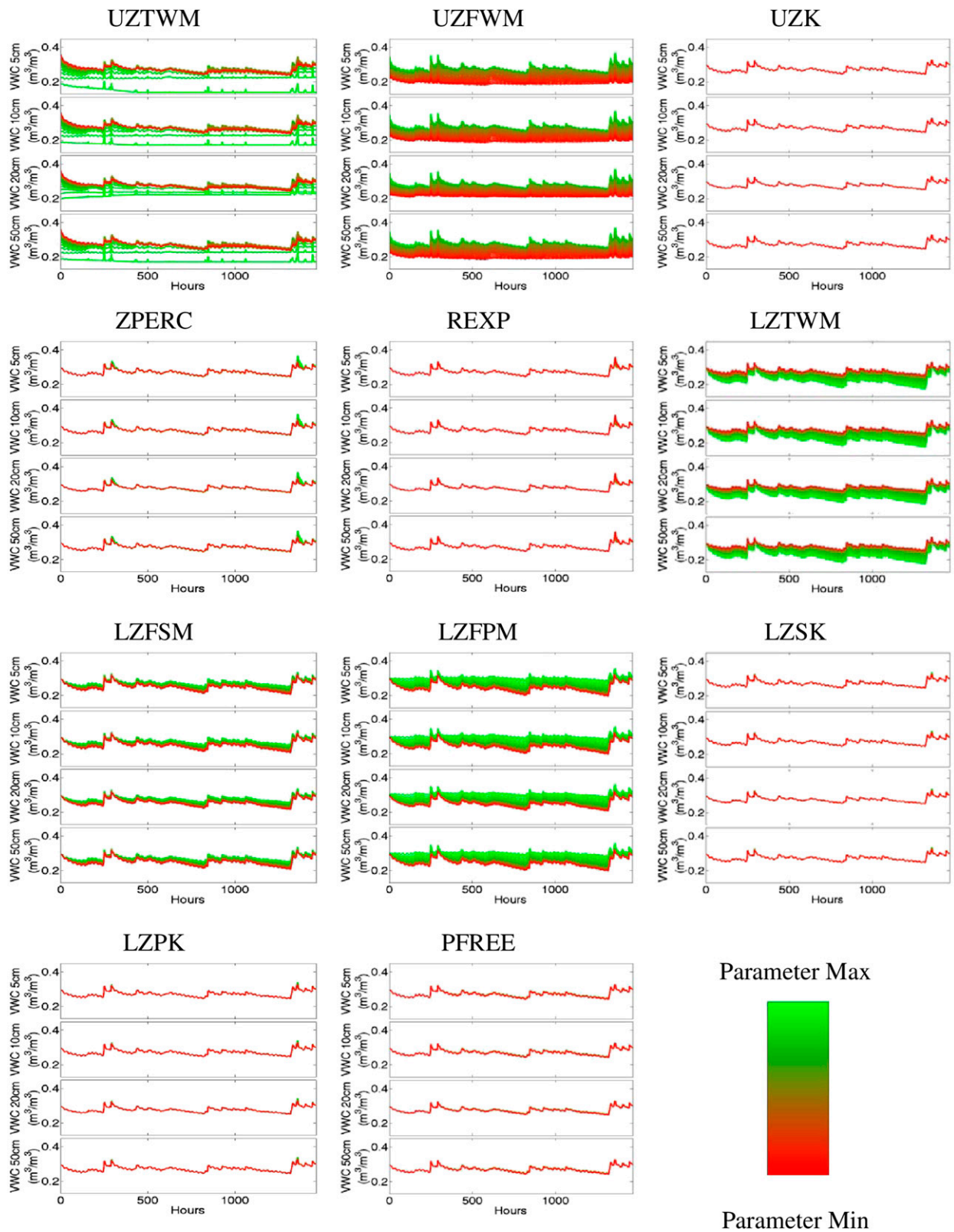
FIG. 5. Soil moisture sensitivity at the four IFloodS sensor depths to individually changed parameters at the single-pixel scale.
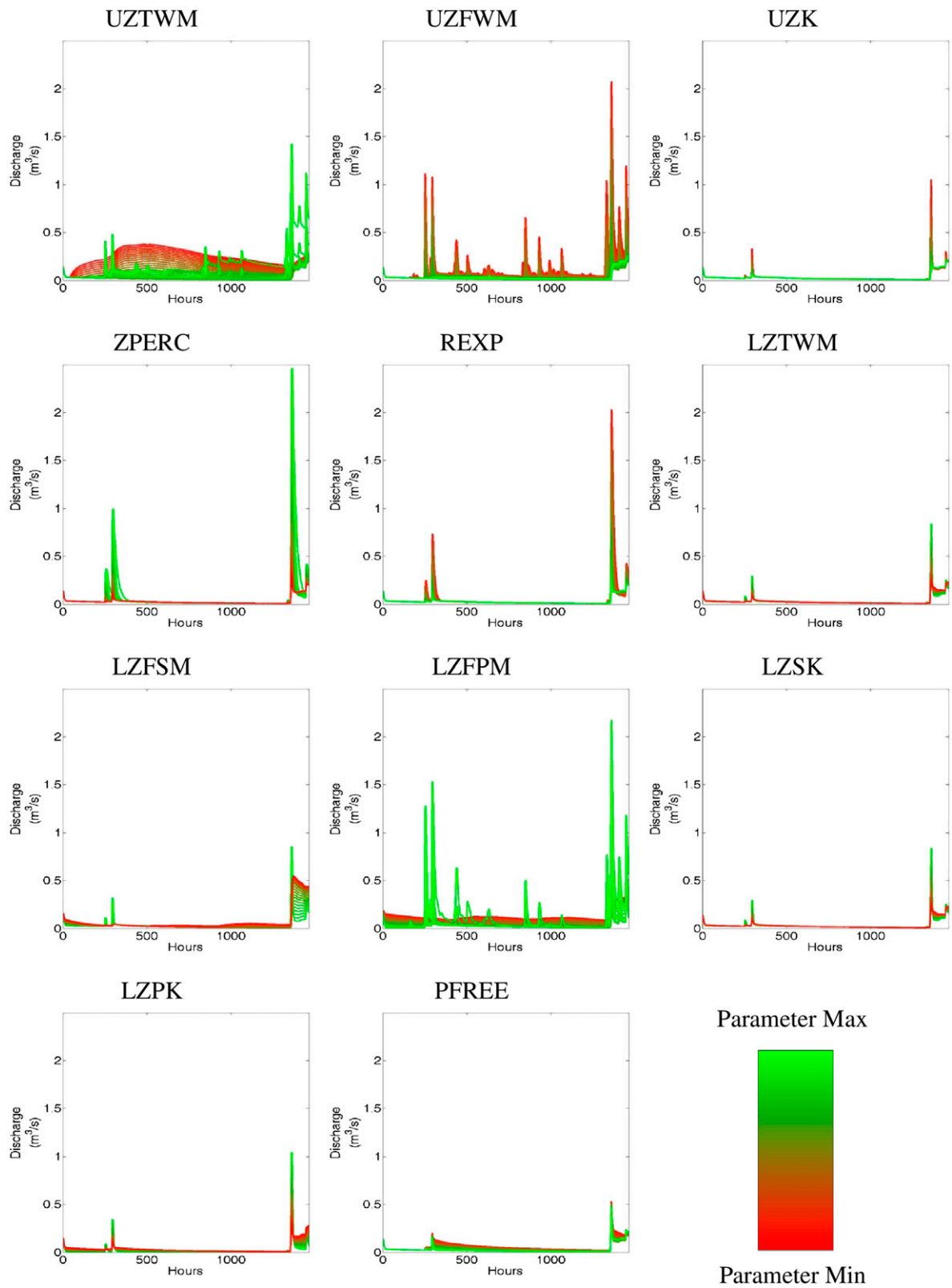
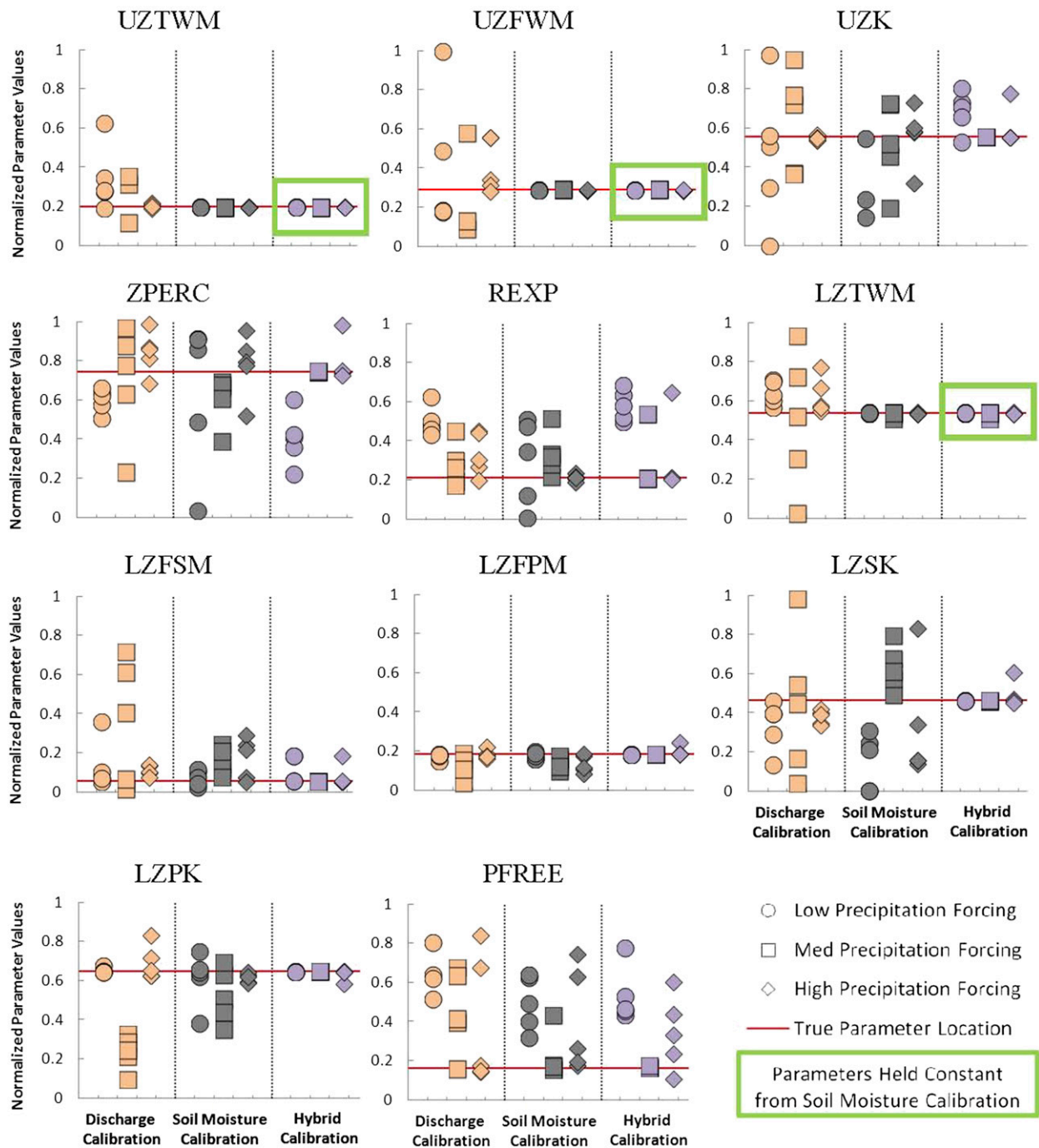FIG. 6. Discharge sensitivity to individually changed parameters at the single-pixel scale.

FIG. 7. Parameter identification tests using synthetic data for a single pixel with discharge-based (orange), soil moisture–based (gray), and hybrid (purple) calibration schemes.

UZK and UZTWM are consistently identified as being close to the true value. Given many intense precipitation events, UZTWM will likely reach its capacity multiple times, allowing for its identification, and since UZK controls the release of quick flow, it too has the necessary conditions for identification. Complementing the rationale of Hogue et al. (2000, 2003), who used low-flow hydrograph segments to calibrate lower-zone parameters, is the precise identification of LZFPM, LZFSM, and LZPK during low precipitation intensity trials. The results of these first two trials are consistent with the findings of Wanders et al. (2014), who found that
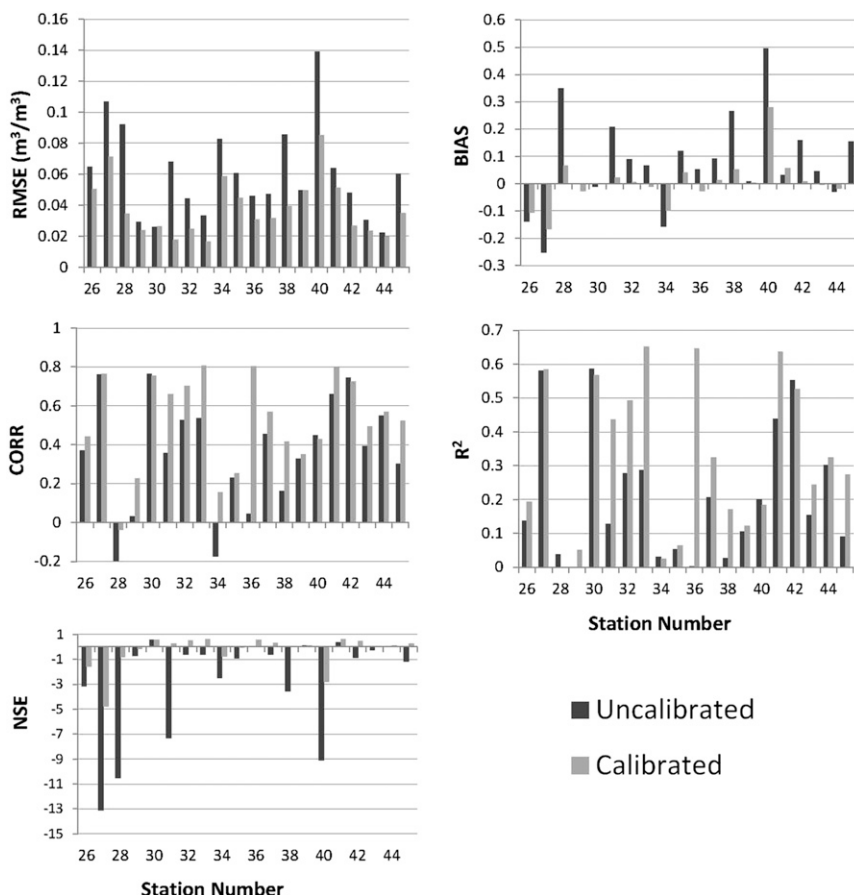
FIG. 8. Statistics of simulated soil moisture at the 20 IFloodS sites before and after individual calibration.

discharge-based calibration was most useful for identifying parameters related to groundwater and routing whereas soil moisture–based calibration had the most positive effect on parameters related to land surface processes. A similar connection is apparent in this experiment with the relationship that soil moisture observations have to surficial processes and ET, as represented by the upperzone and tension water storages, respectively. Furthermore, the discharge observations are able to provide information on groundwater and flow timing, as regulated by the lower-zone and release parameters.

The final calibration case features a two-step hybrid scheme that attempts to combine the strengths of each of the first two cases. Step one is simply case one, where all 11 parameters are allowed to be calibrated to find the lowest soil moisture RMSE. In step two, those parameters that are clearly and consistently identified by soil moisture calibration (i.e., UZTWM, UZFWM, and LZTWM) are held constant and the remaining eight parameters are allowed to be calibrated according to discharge RMSE (purple markers in Fig. 7). Compared to the first two cases, the

hybrid scheme is able to more accurately and precisely identify the prescribed true parameter values with the exception of PFREE and low intensity precipitation forcing trials for UZK, REXP, and ZPERC.

5. Full-basin tests

a. Calibration distribution soil moisture analysis

The 20 HL-RDHM pixels collocated with the soil moisture observations were individually calibrated using SCE-UA. Figure 8 highlights the simulated soil moisture time series statistics before and after each pixel was calibrated. Average improvement in RMSE over a priori values after calibration is 33% with a range of 0%–71%. Improvement in bias, CORR, and R^2 is also seen for nearly all of the observation sites. All sites show an improvement of NSE over the uncalibrated simulations, although 8 of the 20 stations maintain a negative NSE value after calibration, which is unsatisfactory for this metric.
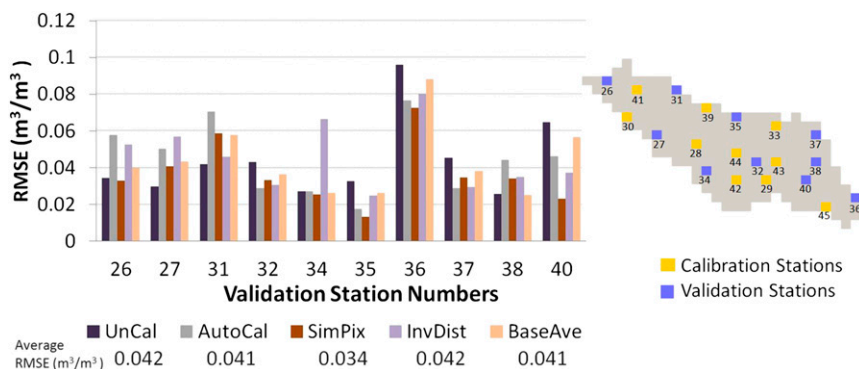
Fig. 9. (left) Soil moisture RMSE at the 10 IFloodS sites used for validation. (right) Map of stations used for soil moisture calibration and validation.

Extending the single-pixel calibration schemes outlined in the previous section to the full-basin scale first requires interpolation of the calibration at the pixels collocated with soil moisture observations to the remaining pixels. Simulations using parameter sets derived from the three distribution methods outlined in section 2b were tested using the IFloodS soil moisture sites. To evaluate soil moisture simulation performance, calibrated parameters from 10 of the sites were used for distribution while the remaining 10 sites were reserved for validation. The observations were distributed to the full-basin scale through inverse distance weighting, which makes it necessary to divide the stations for the two purposes, as the segregation alleviates any advantage the InvDist method would gain from having a weight scheme corresponding perfectly with observation location. In addition to soil moisture simulations from the three soil-moisture-calibration-based schemes, simulated soil moisture using a priori parameters (UnCal) as well as the simulation results using discharge-only-based calibration (AutoCal) were evaluated.

The pixel-based RMSE for each of the five simulations is highlighted in Fig. 9 along with a configuration of which sites were used for calibration–validation and an average RMSE of the 10 validation station simulations under each calibration scheme. The RMSE values presented represent an RMSE of the four soil moisture layers concatenated together into one time series. Of the three soil moisture–based calibration experiments, the SimPix configuration showed the best performance in terms of RMSE (Fig. 10). The central part of the basin exhibits a slight degradation for the SimPix RMSE compared to the UnCal run, but the high RMSE in the southeastern portion of the basin seen in the UnCal simulation experienced the greatest reduction for the SimPix run. The InvDist method showed some degradation in the western basin while the AutoCal and BaseAve simulations

had higher RMSE in the northwestern portion of the basin compared to the UnCal simulation with a slight RMSE reduction in the southeastern region. Considering the collection of 10 validation pixels that are collocated with observations and are not subject to a possibly flawed form of observation interpolation, the SimPix method has the lowest RMSE at five out of the 10 station pixels and has the lowest average RMSE of the five methods tested.

b. Full-basin-calibration streamflow analysis

Based on the results from the calibration distribution tests in section 5a, the SimPix method was selected as the most suitable means for representing a distributed calibration through soil moisture. Therefore, the parameter grids for UZTWM, UZFWM, and LZTWM derived from the SimPix scheme were held constant and the remaining parameters were calibrated using discharge and SCE-UA to form the hybrid calibration scheme. This time, all 20 calibrated pixels were used in the parameter distribution to maximize the potential benefit of the soil moisture calibration. For both the discharge-based and hybrid calibration methods, routing parameters were now allowed to be adjusted during the SCE-UA process.

Figure 11 shows the streamflow simulation results during the analysis period that follows the 1-yr spinup for the various calibration methods. In addition to the discharge-based and hybrid methods, the a priori (default) parameters and calibration using only soil moisture were evaluated. The most notable improvement over the a priori simulation exhibited by the other three simulations is in the reduction of bias (Table 2). The discharge-based, soil moisture–based, and hybrid calibration simulations resulted in a 79%, 45%, and 59% bias reduction, respectively. It is worth noting, however, that all calibrated simulations now underestimate larger peaks while overestimating lower flows for most
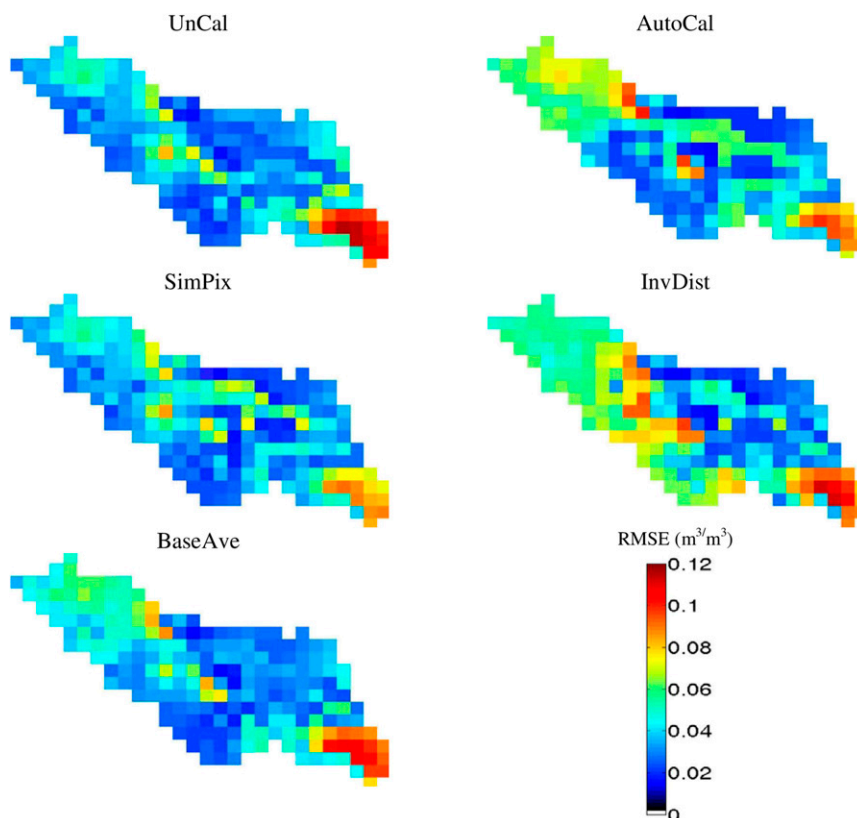
FIG. 10. Distributed basin soil moisture RMSE using 10 IFloodS stations for calibration and 10 for validation.

of the evaluation period. Marked improvement in hydrograph RMSE also resulted from all three calibration efforts with a 42%, 28%, and 35% RMSE reduction for the discharge-based, soil moisture–based, and hybrid calibration simulations, respectively. In terms of the RMSE performance of each simulation relative to one another, the discharge-based calibration showed the greatest improvement over the uncalibrated run, followed by the hybrid calibration scheme, then the soil moisture–based calibration simulation. This pattern of improvement follows the degree of freedom each calibration scheme has compared to the others. An increase in CORR and R^2 for the discharge-based and hybrid calibration methods is shown, with the soil moisture–based calibration method CORR and R^2 being nearly equal to that of the simulation with default parameter sets. These results are aligned with the fact that the soil moisture–based calibration method does not address any routing parameters and thus does not have the freedom to adjust hydrograph features such as peak timing like the discharge-based and hybrid schemes. The NSE of all calibrated simulations improved over the uncalibrated simulation, going from no predictive skill

(negative NSE) to 0.49, 0.23, and 0.37 for discharge based, soil moisture based, and hybrid, respectively.

6. Validation via streamflow

Validation by means of streamflow was done to supplement the lack of soil moisture observations and to also investigate how each calibration process translates to other parts of the water cycle besides soil moisture. The three wet late spring to early summer events for the Turkey River basin used include from 1 April to 10 June 2009, 1 June to 30 July 2010, and 5 April to 5 July 2014 (Fig. 12). In terms of observed hydrographs, the 2009

TABLE 2. Statistics of simulated streamflow for the IFloodS period used for calibration.

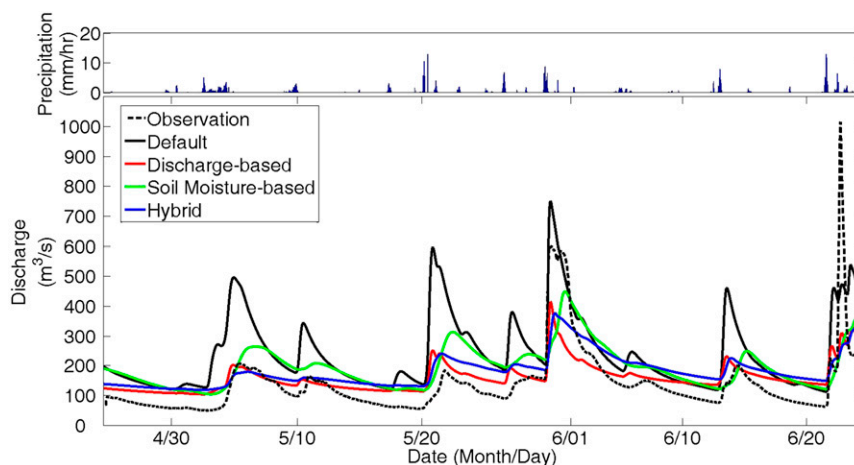| Calibration method	RMSE (m^3 s^{-1})	Bias	CORR	R^2	NSE
April–June 2013					
Default (uncalibrated)	136.14	0.73	0.71	0.51	−0.50
Discharge based	79.22	0.15	0.82	0.67	0.49
Soil moisture based	97.91	0.40	0.70	0.49	0.23
Hybrid	88.62	0.30	0.77	0.59	0.37

FIG. 11. USGS observed discharge and model results for the 2013 IFloodS period used for calibration with basin-average hourly precipitation from stage IV.

event featured a peak smaller than the magnitude of the calibration period peaks, and the 2010 and 2014 events showed peaks roughly equal to the calibration period.

The simulations calibrated with soil moisture showed an 8%–16% reduction in RMSE and the hybrid simulations had an 8%–15% RMSE reduction (Table 3). For the discharge-based calibrated simulations, the RMSE shows an increase from the uncalibrated run for the 2010 event, but a 44% and 18% reduction for 2009 and 2014, respectively. No consistent bias reduction was achieved for any of the three calibration schemes. Correlations remained high for all three validation events and for all simulations calibrated or not (values ranged from 0.84 to 0.98) and R^2 values followed suit (values from 0.70 to 0.96). Gains from calibration over the uncalibrated run in terms of NSE were mostly positive save the discharge-based scheme for the 2010 event. As all calibration efforts were based on RMSE, the improvement seen over the a priori set is anticipated in this metric. Not one calibration method can be classified as "superior" to the others in terms of streamflow simulation given the validation statistics, and in fact, the uncalibrated simulations show the best statistics in some instances.

7. Discussion and conclusions

In this research, the use of concentrated in situ soil moisture observations for calibration of a distributed hydrologic model was investigated through the aid of data from the soil moisture network of the IFloodS field campaign. Calibration of HL-RDHM pixels collocated with the IFloodS soil moisture sensors was performed using the SCE-UA global search algorithm.

A suite of synthetic single-pixel experiments was carried out in order to 1) identify which conceptual parameters had the greatest impact on physically meaningful soil moisture and 2) establish with what procedures (if any) can prescribed conceptual parameters be retrieved using SCE-UA when forced with "perfect" precipitation and temperature and given "perfect" observations. Through a sensitivity analysis of the 11 storage and release parameters, it was found that simulated soil moisture estimates at the four observable physical soil layers were sensitive to changes of storages parameters (UZTWM, UZFWM, LZTWM, LZFPM, and LZFSM), whereas discharge showed some degree of sensitivity to changes in all storage and release parameters.

It was found that UZTWM, UZFWM, and LZTWM could be consistently and precisely identified in the ideal synthetic case using soil moisture RMSE as the objective function. The choice of objective function plays a role in which parameters were more identifiable. Because RMSE targets overall error, adjusting the storage parameters will be most effective in its reduction. It is anticipated that calibrating to an objective function that takes into account how the soil moisture signature is changing (i.e., CORR or NSE) would have more of an impact on some of the release parameters. The identifiability of these three parameters over the others also arises due in part to the location of the observations. With the top three observation layers within the upper zone, there are three time series providing information related to UTZWM and UZFWM. There is some information available to account for LZTWM, with the deepest observation layer representing an area of the soil column between the upper and lower zones. It is likely that had the deepest observation layer not fallen

TABLE 3. Statistics of simulated streamflow for the three validation events.

Calibration method	RMSE (m^3 s^{-1})	Bias	CORR	R^2	NSE
From 1 Apr to 10 Jun 2009					
Default (uncalibrated)	41.08	0.46	0.87	0.75	0.01
Discharge based	22.94	0.39	0.98	0.96	0.69
Soil moisture based	37.59	0.58	0.84	0.70	0.17
Hybrid	37.62	0.68	0.95	0.90	0.17
From 1 Jun to 20 Jul 2010					
Default (uncalibrated)	59.89	−0.01	0.90	0.82	0.63
Discharge based	69.46	−0.40	0.88	0.78	0.50
Soil moisture based	50.23	−0.01	0.87	0.75	0.74
Hybrid	55.19	−0.11	0.86	0.75	0.68
From 5 Apr to 5 Jun 2014					
Default (uncalibrated)	73.98	0.53	0.95	0.91	0.52
Discharge based	60.56	0.19	0.87	0.76	0.68
Soil moisture based	64.34	0.53	0.95	0.89	0.63
Hybrid	63.15	0.49	0.93	0.87	0.65

partly in the area reserved for the lower zone, LZTWM may not have been as easily identified. This should be taken into consideration if only shallow observations are available. The development of the two-step hybrid calibration process led to more consistent parameter identification for all 11 storage and release parameters compared to calibration based solely on soil moisture or discharge.

This work also evaluated the ability of soil moisture–based calibrated simulations to capture streamflow patterns at the full-basin scale. Several advantages of using soil moisture for calibration emerge from this experiment. Soil moisture–based calibration consistently showed improvement in simulated discharge RMSE for both calibration and validation experiments. As the soil moisture calibration had no connection to routing parameters, peak timing could not be improved, but peak magnitude was improved in most cases. Additionally, the realized reduction in streamflow RMSE for soil moisture–based calibrated simulations was achieved even with a calibration time period that is a fraction of what has been deemed necessary for stability when calibrating with streamflow. Given that calibration was performed for a single, multimonth time period, events for validation through streamflow were selected to be similar to conditions during the IFloodS campaign. Yapo et al. (1996) conclude that approximately 8 years of observed streamflow are required for a relatively stable calibration. However, to satisfy the goal to calibrate within the limited time frame of the IFloodS campaign for both the soil moisture and the streamflow-based schemes, this recommendation is unattainable. Wet late spring to early summer events (similar to IFloodS conditions) of three other years were selected

for validation in an effort to compensate for the lack in the observation record. It is acknowledged that to expect high model performance, especially from the calibration schemes involving discharge, is unreasonable for conditions too dissimilar to the short calibration period. While much more investigation is needed, it may be so that less time is required to find stable parameters when calibrating with soil moisture. Given observations with a longer time period, it would be worth following the example of Yapo et al. (1996) to test what kind of calibration time length is required for soil moisture–based calibration. This would provide a more thorough account of how the dual calibration of soil moisture and streamflow can be merged together.

Even though RMSE was reduced for nearly all of the calibration–validation period calibrated streamflow simulations, the overall performance in terms of capturing streamflow patterns begs the question of whether or not any one (or any) of the calibration methods can be considered satisfactory. It is certainly worth exploring whether or not extending the streamflow calibration period can enhance performance within the scope of the other evaluation metrics (particularly for the discharge-based and hybrid calibration schemes). Furthermore, this study focuses strictly on the minimization of RMSE during calibration, which puts emphasis on reducing magnitude of errors over matching hydrograph evolution. It is possible that a multivariable, multiobjective approach that takes into account the shape of the observed hydrograph compared to the simulation (NSE, for example) could enhance the performance of the streamflow simulated with calibrated parameters. While it is not clear from this experiment that soil moisture–based or hybrid calibration of HL-RDHM can greatly enhance streamflow prediction, the added information provided by soil moisture in the calibration process improves soil moisture estimates in a distributed sense rather than scalar improvement of the basin average. Individual pixel calibration had an average improvement of 33% reduction of RMSE. This feature allows for adjustment in the representation of basin heterogeneity if needed, which is a feat that discharge-only-based calibration is unable to achieve. Other studies have shown improvement in streamflow simulation using soil moisture for calibration (i.e., Campo et al. 2006; Wanders et al. 2014), so this objective appears obtainable through additional exploration.

When considering the possibilities of calibrating ungauged basins or those with limited observations, soil moisture–based calibration becomes an attractive option. This is especially relevant with the availability of global soil moisture observations through satellite-based
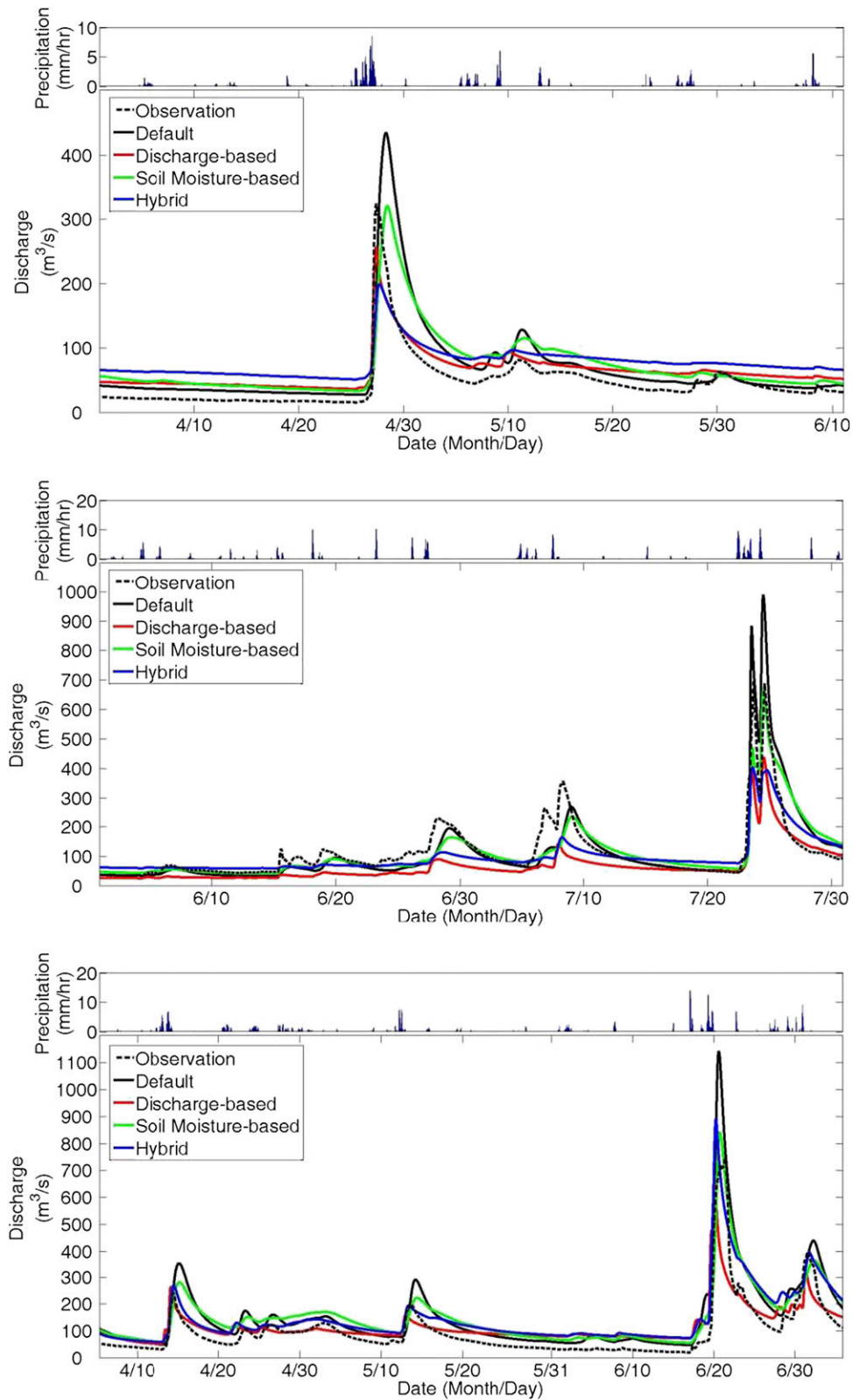
FIG. 12. USGS observed discharge and model results for three validation events (from top to bottom: 2009, 2010, and 2014) with basin-average hourly precipitation from stage IV.

estimates such as SMAP and SMOS. However, when considering satellite-retrieved soil moisture, certain adaptations may be necessary because only the top-layer soil moisture is available (which may reduce meaningful connection to LZTWM) and that the temporal resolution is on the daily to multiday scale rather than hourly.

The complex geology and topography of the basin itself presents a unique challenge in the context of this experiment. High soil moisture RMSE values in the southeastern part of the Turkey River basin (Fig. 10) reveal themselves in a pattern that coincides well with the highly karstic areas highlighted in Fig. 2. Currently, HL-RDHM is not formulated to directly take into account the effect that these types of formations have. It is possible that having distributed observations such as soil moisture to calibrated can help separate out problematic areas and define proper parameter values, at least in areas that are less karstic and that conform to the type of processes HL-RDHM can handle. This is opposed to the alternative of trying to distinguish what portion of the hydrograph behavior is attributed to the karstic regions.

Several conclusions can be drawn from this study. Synthetic experiments fed with perfect observations revealed that three storage parameters were strongly identifiable through soil moisture calibration and that all 11 parameters were more recoverable when used in a two-step hybrid calibration with observed discharge than calibration to either variable individually. Of the three calibration distribution methods, it was found that the SimPix method, defined on the principle of a given uncalibrated pixel's similarity to the calibrated pixels, was the most appropriate for use in distributing the calibration effects. The inclusion of soil moisture observations in the calibration process was able to consistently reduce RMSE and increase NSE of simulated streamflow, which discharge-based calibration could not do given such a short calibration period. However, the mixed results of other evaluation metrics suggest that more investigation is needed before soil moisture–based calibration can be confidently used by itself to improve streamflow estimation with HL-RDHM.

REFERENCES

Anderson, E., 1973: National Weather Service River Forecast System–Snow accumulation and ablation model. NOAA Tech. Memo. NWS HYDRO-17, 87 pp. [Available online at ftp://ftp.wcc.nrcs.usda.gov/wntsc/H&H/snow/AndersonHYDRO17.pdf.]

Bergström, S., G. Lindström, and A. Pettersson, 2002: Multi-variable parameter estimation to increase confidence in hydrological modeling. *Hydrol. Processes*, **16**, 413–421, doi:10.1002/hyp.332.

Brazil, L. E., and M. D. Hudlow, 1981: Calibration procedures used with the National Weather Service Forecast System. *Water and Related Land Resources*, Y. Y. Haimes and J. Kindler, Eds., Pergamon, 457–466.

Brock, F., K. Crawford, R. Elliott, G. Cuperus, S. Stadler, H. Johnson, and M. Eilts, 1995: The Oklahoma Mesonet: A technical overview. *J. Atmos. Oceanic Technol.*, **12**, 5–19, doi:10.1175/1520-0426(1995)012<0005:TOMATO>2.0.CO;2.

Campo, L., F. Caparrini, and F. Castelli, 2006: Use of multi-platform, multi-temporal remote-sensing data for calibration of a distributed hydrological model: An application in the Arno basin, Italy. *Hydrol. Processes*, **20**, 2693–2712, doi:10.1002/hyp.6061.

Cao, W., W. Bowden, T. Davie, and A. Fenemor, 2006: Multi-variable and multi-site calibration and validation of SWAT in a large mountainous catchment with high spatial variability. *Hydrol. Processes*, **20**, 1057–1073, doi:10.1002/hyp.5933.

Chen, F., and coauthors, 1996: Modeling of land surface evaporation by four schemes and comparison with FIFE observations. *J. Geophys. Res.*, **101**, 7251–7268, doi:10.1029/95JD02165.

Chu, W., X. Gao, and S. Sorooshian, 2010: Improving the shuffled complex evolution scheme for optimization of complex nonlinear hydrological systems: Application to the calibration of the Sacramento soil-moisture accounting model. *Water Resour. Res.*, **46**, W09530, doi:10.1029/2010WR009224.

Cooper, V., V. Nguyen, and J. Nicell, 1997: Evaluation of global optimization methods for conceptual rainfall–runoff model calibration. *Water Sci. Technol.*, **36**, 53–60, doi:10.1016/S0273-1223(97)00461-7.

——, ——, and ——, 2007: Calibration of conceptual rainfall–runoff models using global optimization methods with hydrologic process-based parameter constraints. *J. Hydrol.*, **334**, 455–466, doi:10.1016/j.jhydrol.2006.10.036.

Das, N., B. Mohanty, M. Cosh, and T. Jackson, 2008: Modeling and assimilation of root zone soil moisture using remote sensing observation in Walnut Gulch Watershed during SMEX04. *Remote Sens. Environ.*, **112**, 415–429, doi:10.1016/j.rse.2006.10.027.

Demir, I., and Coauthors, 2015: Data-enabled field experiment planning, management, and research using cyberinfrastructure. *J. Hydrometeor.*, **16**, 1155–1170, doi:10.1175/JHM-D-14-0163.1.

Downer, C., and F. Ogden, 2004: GSSHA: Model to simulate diverse stream flow producing processes. *J. Hydrol. Eng.*, **9**, 161–174, doi:10.1061/(ASCE)1084-0699(2004)9:3(161).

Duan, Q., S. Sorooshian, and V. Gupta, 1992: Effective and efficient global optimization for conceptual rainfall–runoff models. *Water Resour. Res.*, **28**, 1015–1031, doi:10.1029/91WR02985.

——, ——, and ——, 1994: Optimal use of the SCE-UA global optimization method for calibrating watershed models. *J. Hydrol.*, **158**, 265–284, doi:10.1016/0022-1694(94)90057-4.

Entekhabi, D., and Coauthors, 2010: The Soil Moisture Active Passive (SMAP) mission. *Proc. IEEE*, **98**, 704–716, doi:10.1109/JPROC.2010.2043918.

Fares, A., R. Awal, J. Michaud, P.-S. Chu, S. Fares, K. Kodama, and M. Rosener, 2014: Rainfall–runoff modeling in a flashy tropical watershed using the distributed HL-RDHM model. *J. Hydrol.*, **519**, 3436–3447, doi:10.1016/j.jhydrol.2014.09.042.

Franz, K. J., and L. Karsten, 2013: Calibration of a distributed snow model using MODIS snow covered area data. *J. Hydrol.*, **494**, 160–175, doi:10.1016/j.jhydrol.2013.04.026.

Gan, T., and G. Biftu, 1996: Automatic calibration of conceptual rainfall–runoff models: Optimization algorithms, catchment conditions, and model structure. *Water Resour. Res.*, **32**, 3513–3524, doi:10.1029/95WR02195.

Gupta, H., S. Sorooshian, and P. Yaop, 1998: Toward improved calibration of hydrologic models: Multiple and noncommensurable measures of information. *Water Resour. Res.*, **34**, 751–763, doi:10.1029/97WR03495.

Hogue, T., S. Sorooshian, and H. Gupta, 2000: A multistep automatic calibration scheme for river forecasting models. *J. Hydrometeor.*, **1**, 524–542, doi:10.1175/1525-7541(2000)001<0524:AMACSF>2.0.CO;2.

——, H. Gupta, S. Sorooshian, and C. Tomkins, 2003: A multi-step automatic calibration scheme for watershed models. *Calibration of Watershed Models*, Q. Duan et al., Eds., Water Science and Application Series, Vol. 6, Amer. Geophys. Union, 165–174.

Hsu, K., J. Li, and S. Sorooshian, 2012: To improve model soil moisture estimation in arid/semi-arid region using in situ and remote sensing information. *Paddy Water Environ.*, **10**, 165–173, doi:10.1007/s10333-011-0308-9.

Immerzeel, W., and P. Droogers, 2008: Calibration of a distributed hydrological model based on satellite evapotranspiration. *J. Hydrol.*, **349**, 411–424, doi:10.1016/j.jhydrol.2007.11.017.

Isenstein, E., S. Wi, and Y. E. Yang, 2015: Calibration of a distributed hydrologic model using streamflow and remote sensing snow data. *World Environmental and Water Resources Congress 2015*, K. Karvazy and V. L. Webster, Eds., ASCE, 973–982, doi:10.1061/9780784479162.093.

Ivanov, V., S. Fatichi, G. Jenerette, J. Espeleta, P. Troch, and T. Huxman, 2010: Hysteresis of soil moisture spatial heterogeneity and the ''homogenizing'' effect of vegetation. *Water Resour. Res.*, **46**, W09521, doi:10.1029/2009WR008611.

Keefer, T., M. Moran, and G. Paige, 2008: Long-term meteorological and soil hydrology database, Walnut Gulch Experimental Watershed, Arizona, United States. *Water Resour. Res.*, **44**, W05S07, doi:10.1029/2006WR005702.

Kerr, Y., and Coauthors, 2010: The SMOS mission: New tool for monitoring key elements of the global water cycle. *Proc. IEEE*, **98**, 666–687, doi:10.1109/JPROC.2010.2043032.

Koren, V., M. Smith, and Q. Duan, 2003: Use of a priori parameter estimates in the derivation of spatially consistent parameter sets of rainfall–runoff models. *Calibration of Watershed Models*, Q. Duan et al., Eds., Water Science and Application Series, Vol. 6, Amer. Geophys. Union, 239–254.

——, S. Reed, M. Smith, Z. Zhang, and D. J. Seo, 2004: Hydrology laboratory research modeling system (HL-RMS) of the US National Weather Service. *J. Hydrol.*, **291**, 297–318, doi:10.1016/j.jhydrol.2003.12.039.

——, M. Smith, Z. Cui, and B. Cosgrove, 2007: Physically-based modifications to the Sacramento Soil Moisture Accounting model: Modeling the effects of frozen ground on the rainfall–runoff process. NOAA Tech. Rep. NWS 52, 43 pp. [Available online at www.nws.noaa.gov/oh/hrl/hsmb/docs/hydrology/PBE_SAC-SMA/NOAA_Technical_Report_NWS_52.pdf.]

——, F. Moreda, and M. Smith, 2008: Use of soil moisture observations to improve parameter consistency in watershed calibration. *Phys. Chem. Earth*, **33**, 1068–1080, doi:10.1016/j.pce.2008.01.003.

——, M. Smith, Z. Cui, B. Cosgrove, K. Werner, and R. Zamora, 2010: Modification of Sacramento Soil Moisture Accounting Heat Transfer Component (SAC-HT) for enhanced evapotranspiration. NOAA Tech. Rep. NWS 53, 66 pp. [Available online at http://amazon.nws.noaa.gov/articles/HRL_Pubs_PDF_May12_2009/New_Scans_June_2011/NOAA_Technical_Report_NWS_53.pdf.]

Krajewski, W., B. Seo, R. Goska, I. Demir, and M. Elsaaadani, 2013: Precipitation datasets the GPM Iowa Flood Studies (IFloodS) field experiment. *Geophysical Research Abstracts*, Vol. 15, Abstract EGU2013-22303. [Available online at http://meetingorganizer.copernicus.org/EGU2013/EGU2013-11303.pdf.]

Liang, X., and Z. Xie, 2001: A new surface runoff parameterization with subgrid-scale soil heterogeneity for land surface models. *Adv. Water Resour.*, **24**, 1173–1193, doi:10.1016/S0309-1708(01)00032-X.

Libra, R., 2005: Living in Karst. Iowa Geological Survey Guidebook Series, No. 25, Iowa Dept. of Natural Resources, 48 pp. [Available online at https://s-iihr34.iihr.uiowa.edu/publications/uploads/GB-25.pdf.]

Moriasi, D. N., J. G. Arnold, M. W. Van Liew, R. L. Bingner, R. D. Harmel, and T. L. Veith, 2007: Model evaluation guidelines for systematic quantification of accuracy in watershed simulations. *Trans. ASABE*, **50**, 885–900, doi:10.13031/2013.23153.

Nguyen, P., A. Thorstensen, S. Sorooshian, K. Hsu, and A. AghaKouchak, 2015: Flood forecasting and inundation mapping using HiResFlood-UCI and near-real-time satellite precipitation data: The 2008 Iowa flood. *J. Hydrometeor.*, **16**, 1171–1183, doi:10.1175/JHM-D-14-0212.1.

NWS, 2011: Hydrology Laboratory-Research Distributed Hydrologic Model (HL-RDHM) user manual, version 3.2.0. NWS Rep., 131 pp.

Rientjes, T., L. Muthuwatta, M. Bos, M. Booij, and H. Bhatti, 2013: Multi-variable calibration of a semi-distributed hydrological model using streamflow data and satellite-based evapotranspiration. *J. Hydrol.*, **505**, 276–290, doi:10.1016/j.jhydrol.2013.10.006.

Robinson, D., 1990: The United States Cooperative Climate-Observing systems: Reflections and recommendations. *Bull. Amer. Meteor. Soc.*, **71**, 826–831, doi:10.1175/1520-0477(1990)071<0826:TUSCCO>2.0.CO;2.

Santanello, J., Jr., C. Peters-Lidard, M. Garcia, D. Mocko, M. Teschler, M. Moran, and D. Thoma, 2007: Using remotely-sensed estimates of soil moisture to infer soil texture and hydraulic properties across a semi-arid watershed. *Remote Sens. Environ.*, **110**, 79–97, doi:10.1016/j.rse.2007.02.007.

Schaefer, G., M. Cosh, and T. Jackson, 2007: The USDA Natural Resources Conservation Service Soil Climate Analysis Network (SCAN). *J. Atmos. Oceanic Technol.*, **24**, 2073–2077, doi:10.1175/2007JTECHA930.1.

Schwaller, M., and K. Morris, 2011: A ground validation network for the Global Precipitation Measurement Mission. *J. Atmos. Oceanic Technol.*, **28**, 301–319, doi:10.1175/2010JTECHA1403.1.

Scott, B., T. Ochsner, B. Illston, C. Fiebrich, J. Basara, and A. Sutherland, 2013: New soil property database improves Oklahoma Mesonet soil moisture estimates. *J. Atmos. Oceanic Technol.*, **30**, 2585–2595, doi:10.1175/JTECH-D-13-00084.1.

Shafii, M., and F. De Smedt, 2009: Multi-objective calibration of a distributed hydrological model (WetSpa) using a genetic algorithm. *Hydrol. Earth Syst. Sci.*, **13**, 2137–2149, doi:10.5194/hess-13-2137-2009.

Smith, M., and Coauthors, 2012: Results of the DMIP 2 Oklahoma experiments. *J. Hydrol.*, **418–419**, 17–48, doi:10.1016/j.jhydrol.2011.08.056.

Sorooshian, S., Q. Duan, and V. Gupta, 1993: Calibration of rainfall–runoff models: Application of global optimization to the Sacramento Soil Moisture Accounting Model. *Water Resour. Res.*, **29**, 1185–1194, doi:10.1029/92WR02617.

Spies, R. R., K. J. Franz, T. S. Hogue, and A. L. Bowman, 2015: Distributed hydrologic modeling using satellite-derived potential evapotranspiration. *J. Hydrometeor.*, **16**, 129–146, doi:10.1175/JHM-D-14-0047.1.

Tapiador, F., and Coauthors, 2012: Global precipitation measurement: Methods, datasets and applications. *Atmos. Res.*, **104–105**, 70–97, doi:10.1016/j.atmosres.2011.10.021.

van Dam, J., J. Huygen, J. Wesseling, R. Feddes, P. Kabat, and P. Van Waslum, 1997: Theory of SWAP version 2.0: Simulation of water and plant growth in the soil–water–atmosphere–plant environment. Rep. 71/Tech. Doc. 45, Wageningen Agricultural University/DLO Winand Staring Centre, 167 pp.

van der Knijff, J., J. Younis, and A. De Roo, 2010: LISFLOOD: A GIS-based distributed model for river basin scale water balance and flood simulation. *Int. J. Geogr. Inf. Sci.*, **24**, 189–212, doi:10.1080/13658810802549154.

Vrugt, J., H. Gupta, L. Bastidas, W. Bouten, and S. Sorooshian, 2003a: Effective and efficient algorithm for multiobjective optimization of hydrologic models. *Water Resour. Res.*, **39**, 1214, doi:10.1029/2002WR001746.

——, ——, W. Bouten, and S. Sorooshian, 2003b: A shuffled complex evolution metropolis algorithm for estimating posterior distribution of watershed model parameters. *Calibration of Watershed Models*, Q. Duan et al., Eds., Water Science and Application Series, Vol. 6, Amer. Geophys. Union, 105–112.

Wanders, N., M. Bierkens, S. de Jong, A. de Roo, and D. Kaarssenberg, 2014: The benefits of using remotely sensed soil moisture in parameter identification of large-scale hydrological models. *Water Resour. Res.*, **50**, 6874–6891, doi:10.1002/2013WR014639.

Wood, E., D. Lettenmaier, and V. Zartarian, 1992: A land-surface hydrology parameterization with subgrid variability for general circulation models. *J. Geophys. Res.*, **97**, 2717–2728, doi:10.1029/91JD01786.

Yapo, P., H. Gupta, and S. Sorooshian, 1996: Automatic calibration of conceptual rainfall–runoff sensitivity to calibration data. *J. Hydrol.*, **181**, 23–48, doi:10.1016/0022-1694(95)02918-4.

——, ——, and ——, 1998: Multi-objective global optimization for hydrologic models. *J. Hydrol.*, **204**, 83–97, doi:10.1016/S0022-1694(97)00107-8.

Zamora, R., F. M. Ralph, E. Clar, and T. Schneider, 2011: The NOAA Hydrometeorology Testbed soil moisture observing networks: Design instrumentation, and preliminary results. *J. Atmos. Oceanic Technol.*, **28**, 1129–1140, doi:10.1175/2010JTECHA1465.1.

——, E. Clark, E. Rogers, M. Ek, and T. Lahmers, 2014: An examination of meteorological and soil moisture conditions in the Babocomari River basin before the flood event of 2008. *J. Hydrometeor.*, **15**, 243–260, doi:10.1175/JHM-D-12-0142.1.

Zhang, C., R. Wang, and Q. Meng, 2015: Calibration of conceptual rainfall–runoff models using global optimization. *Adv. Meteor.*, **2015**, 545376, doi:10.1155/2015/545376.